Construction and Building Materials 414 (2024) 134765

Contents lists available at ScienceDirect

Construction and Building Materials

journal homepage: www.elsevier.com/locate/conbuildmat

Hybrid grouted steel connections using adhesively bonded granules in the steel grout interface: Development and validation of an innovative joining technique

Sebastian Myslicki [a,*], Till Vallée [a], Holger Fricke [a], Thomas Ummenhofer [b], Jakob Boretzki [b], Matthias Albiez [b]

[a] *Fraunhofer Institute for Manufacturing Technology and Advanced Materials IFAM, Wiener Street 12, Bremen, Germany*
[b] *KIT Steel and Lightweight Structures, Otto-Ammann-Platz 1, 76131 Karlsruhe, Germany*

A R T I C L E I N F O

Keywords:
Joining technology
Hybrid joint
Grouted joint
Adhesive bonding
Durability, temperature resistance

A B S T R A C T

This study introduces an innovative hybrid grouted connection method which utilizes organic adhesive with embedded granulates as a bonding agent to connect high strength grout mortar uniformly to smooth steel surfaces. This approach eliminates the need for welding additional shear keys, which are currently used for local form fit. The primary objective is to investigate the general usability of this method, particularly for demanding applications in steel construction. The manufacturing procedure on small-scale specimens is shown by using epoxy-based adhesive tape and paste –like two component epoxies. With help of such small-scale hybrid test specimens, different combinations of grout, adhesive and granulates were tested to qualify the combinations with the highest load-bearing capacity. It could be shown that even when connected to smooth steel surfaces, high loads with a slight scattering could be transferred with help of the adhesive-granulate promoter. Because these types of connections are widely exposed to harsh environmental conditions, further investigations concerning the temperature stability and durability were implemented. Temperature variations within the typical range of offshore structures, namely T = −20 °C as minimum and T = 60 °C as maximum temperature are considered and set into relation to the test results performed at ambient temperature. Temperature variations have a notable effect on load-bearing capacities, with lower temperatures showing a beneficial influence. The results demonstrate the operational capability of the hybrid connections, even at higher temperatures the expected reduction of the load capacity was very modest. Durability has been proven by specimen exposure to artificial seawater and climatic cycling tests produce varying effects. Some samples exhibit an increased load-bearing capacity, indicating further crosslinking of the adhesive, while others show no significant reduction of load-bearing capacity. As fracture patters could verify, both adhesive systems effectively protect against corrosion, as no infiltration of corrosion into the steel-adhesive interface were observed. In conclusion, the hybrid grout connection method, presented in this research offers several advantages over conventional grouting techniques. The ability for high load transfer, temperature stability and durability underline its potential as a reliable alternative for joining steel components in various applications.

1. Introduction

The current method of joining circular hollow sections (CHS) in offshore structures involves the utilization of grout injection mortar and welded shear keys. However, these connection types often result in stress concentrations that can lead to fatigue cracks and damage to the grouting mortar. Furthermore, water ingress and corrosion exacerbate these issues. In order to address these challenges, this study investigates the potential of hybrid grouted connections incorporating organic adhesive interfaces. The mechanical characteristics of the hybrid grouted connection are clearly influenced by the choice of specific grout-adhesive combinations. Hence, a comprehensive study was conducted involving both components to explore the wide range of prioritized adhesives and grout mortars. As the investigated joint type is to be used in structural steel applications, additional tests regarding temperature range and ageing were conducted.

* Corresponding author.
E-mail address: sebastian.myslicki@ifam.fraunhofer.de (S. Myslicki).

https://doi.org/10.1016/j.conbuildmat.2023.134765
Received 2 June 2023; Received in revised form 17 October 2023; Accepted 24 December 2023
Available online 18 January 2024

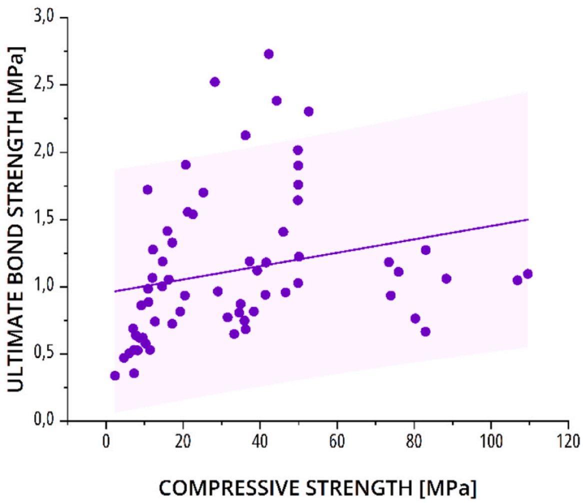

Fig. 1. Relationship between bond strength and compressive strength of grout for plain pipes (redrawn with data from [1]); note the relative low values of the ultimate bond strength, if compared to lap shear strength of usual structural adhesives.

1.1. Grouted connections

Grouted connections are critical parts of the integrity of offshore wind turbine structures since they transfer the load bearing structure to the lower foundations. Grouted joints consist of two steel tubes with different diameters that are connected using grout filling the tubular gap between the tubes. The larger, outer, tube is usually called sleeve, whereas the smaller, inner, one is the pile. In general, the connection can be constructed with or without shear keys. For fixed offshore platforms, usually shear connectors are used to increase the load-bearing capacity. Different load-bearing mechanisms can be distinguished in connections with shear keys: adhesion and friction in the interfaces between grout and steel tubes, and the load-bearing capacity of compression struts between the shear keys on the pile and the sleeve. Enhancements.

in the frictional aspects can improve the performance of the connection significantly, even when shear keys are used. The bond strength in the steel-grout interface was found out to range between 1 and 3 MPa (cf. [1] and Fig. 1). These bond strength values are relatively low compared to typical values achieved with structural adhesives [2–6], which are 5 to 10 times higher. Improving bond strengths would not only increase the average value but also reduce the scatter, leading to more reliable and consistent performance of grouted joints.

It is worth to mentioning, that filling the tubular gap solely with adhesive is no practical alternative, as the load capacity is significantly reduced with higher bonding gaps. Nevertheless, a high amount of adhesive will be required causing undesired exothermal effects and high material costs [7]. The use of an adhesive without the embedding of the granules is not effective due to fundamental load transfer considerations. The load transfer of the hybrid grouted joint is based on the mechanical interlocking of the granules embedded in the adhesive with the not yet cured grout material. Not least for this reason, a grout material with a maximum grain size of 1 mm, which allows good interlocking with the granules is chosen.

The major parameters that characterize the load-deformation behaviour and the maximum load are the ratio of diameter to thickness (D/t) of pile, sleeve, and grout, the compressive strength of the grout, and the ratio of height to spacing (h/s) of the shear keys. The main failure modes of connections with shear keys are shear failure along the shear connectors for too closely spaced shear keys and crushing of the grout on the stressed side of the shear keys for grouted joints with an appropriate shear key spacing. In this case, usually diagonal cracks occur in the grout. Despite having been extensively used in offshore applications over the last decades, recent concerns over insufficient performance of monopile connections in wind farms prompted this paper to review engineering methods and numerical models used for load determination and investigation of structural behaviour [8], with the interface contact considered to be decisive for the structural analysis. Pre-mid 2009 papers reviewed in [9] suggest that inadequate design codes and limited testing under actual loading conditions, confinement, and representative environmental conditions may have caused unexpected issues in large-diameter grouted connections.

The effectiveness of the steel-grout interface has been called into question for several reasons. Specifically, the lower coefficients of friction resulting from water penetration and the grout's susceptibility to grout crushing and flush-out under repeated fatigue loads have raised concerns. New design recommendations [10] for grouted jacket pile-sleeve connections have been proposed based on recent research, with emphasis on robust designs that can withstand cyclic loads on offshore structures, for which current practice, with or without shear keys, appears vulnerable.

Further details on the design of grouted joint connections for offshore wind energy converters and fatigue assessment can be found in [11–13]. These papers specifically address the issue of vertical slippages observed in offshore wind turbines, which result from underestimating the cyclic effects on axial capacity. Through non-linear finite element simulations, the authors demonstrate the progressive vertical misalignment of grouted connections within dynamically loaded structures. The evaluation of parameters affecting long-term axial capacity behaviour reveals the negative impact of mechanical interlock on fatigue performance in grouted joints. Consequently, the poor fatigue performance of mechanical shear keys often necessitates conservative dimensioning and design practices.

In summary, the load-bearing capacity of grouted connections on smooth steel surfaces is severely limited due to the loss of adhesion between the grout and the steel. This occurs due to the necessity for significant displacement of the sleeve relative to the pile in order to activate load transfer. Despite the high efficiency of current grouts, the load-bearing capacity of the mortar remains underutilized. To address this issue, shear keys are applied, leading to the formation of compression struts in the grout layer. However, the use of shear keys leads to local grout crushing in front of the shear keys. This crushing becomes particularly problematic under repeated loading conditions below the water surface, as crushed grout particles are flushed out, demanding complex reinforcement measures to mitigate the issue.

1.2. Adhesively bonded connections

Established joining methods in structural steel are bolting and welding, but adhesive bonding is increasingly being considered as a complement [14], or substitute, even for load transmission [5,15]. The strength of any adhesive bond is limited by the smaller of the cohesive or adhesive strength. Cohesive strength, in a nutshell, is the intrinsic strength the adhesive builds up [16]; it depends on the type of adhesive, the conditions under which it had cured [17], and of the environmental conditions (most notably temperature [18]) under which it is loaded. Adhesive strength [19] mostly depends on the surface conditions prevalent on the surface to be bonded, and the interpenetration of adhesive and adherend plays a crucial role in this process. While the latter is evident at a macro scale for fibrous materials, it is more subtle for metal and metal oxide surfaces, for which surface preparation techniques, ranging from simple degreasing [20], blasting, the use of primers to chemical surface etching, may be required. The relative limited application of adhesives for load bearing joints in the context of structural steel has been summarised in a series of recent papers, e.g. Albiez et al. for adhesively bonded steel tubes [5,15], Albiez et al. for offshore structures [6,21], Yokozeki et al. for hybrid joints involving pre-tensioned bolts [22], and durability of adhesively bonded secondary structures in the context of offshore structures was considered by

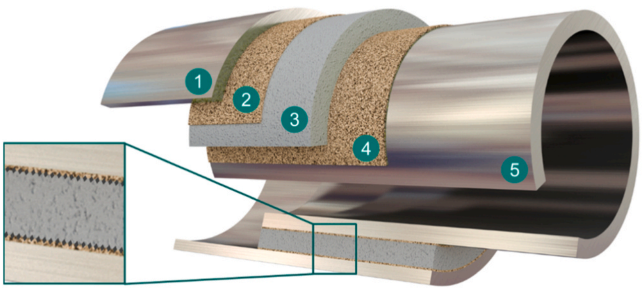

Fig. 2. Concept of a hybrid grout joint: ① Outer tube (sleeve), ② and ④ Adhesive with integrated granulate, ③ grouting mortar, and ⑤ inner tube (pile).

Myslicki et al. [23]. For more information related to adhesive bonding, in particular points not central to this paper, readers are redirected to reference works as [24,25].

1.3. Proposed innovative alternative

Regarding the aforesaid, grouted joints can, to some extent, be conceptualised as adhesively bonded joints, with "cohesive strength" being linked to the compressive strength of the grout, and "adhesive strength" related to the conditions at the grout-steel interface (either smooth or strength obtained by dividing the failure load by the surface area of the interface, which is very similar to what is done in adhesion science. Yet, there are differences in the definition on how grout "adheres" to the sleeve and the pile; the mechanics are often described as friction (and a corresponding coefficient μ), to which a cohesive term (denoted c) may be added. Thus shear strength τ and normal stress σ may be approximated in its simplest for as a Mohr-Coulomb condition [26] or more complex variants thereof [27].

Nevertheless, similar to adhesively bonded joints [28], describing load transfer in grouted joints solely in terms of shear stresses oversimplifies the complex interplay between shear and transverse normal stresses. The intricate nature of the phenomena described above is exemplified by the dual effect of compressive normal stresses, which enhance shear strength, while tensile normal stress undermines it. Thus, the utilization of failure criteria becomes imperative to accurately determine the material strength in such scenarios, an aspect that will be addressed in an upcoming publication.

This manuscript describes the development of a novel hybrid grouted joint for steel structures that employs both grout and adhesive layers in a complementary manner, leveraging the distinctive properties of each material to enhance the joint's overall performance. The hybrid grouted joint introduced in this study is characterized by a multilayer structure, as depicted in Fig. 2. The manufacturing process comprises several stages. Initially, the bonding surfaces of the structural components, sleeve, and pile, are treated with sandblasting and coated with a thin layer of organic adhesive, herein epoxy adhesives, with the bonding process is performed under controlled environmental conditions in a manufacturing plant.

Following this, inorganic granules like corundum or quartz sand are embedded into the yet uncured adhesive. The granules are selected so to protruding significantly from the adhesive layer, i.e., their diameter is twice the adhesive layer thickness. To create a form-fit, a high-strength grout is then poured into the remaining gap, which interlocks with the inorganic granules along the entire surface. The rough and coarse surface of the adhesive-granule modified surfaces enables efficient and uniform load transfer into the grout, which has the potential to prevent local grout crushing and significantly delay fatigue cracks in the steel components. One can conceptualise the proposed approach as replacing the discrete relatively large sized shear keys with almost continuously distributed small granules protruding into the grout material.

2. Materials and methods

2.1. Materials

The concept of the proposed hybrid grouted joint, displayed in Fig. 2 and briefly introduced above, involves four materials: adhesive as the central novel element, grout material, granules and lastly steel for the sleeve and pile (outer and inner tubes). For the proposed hybrid joint to fulfil the expectations, appropriate adhesives had to be selected according to a set of requirements formulated by a panel of designers. The requirements were the following: Adhesives with at least 2′000 MPa E-modulus and not prone to creep are prioritized. The selected adhesive system must withstand temperatures from –8 °C to + 57 °C, according to a previous study [6] in a similar geographical setting, and exhibit a glass transition temperature of at least 60 °C. A pot life of 60 min is necessary based upon estimates of the time needed for manufacturing.

2.1.1. Adhesives

Based on the given requirements, the two adhesives Sikadur-370 and DuploTEC 10490 SBF have been identified as promising options based on their respective technical datasheets (TDS).

The application methods of the Sikadur-370 and DuploTEC 10490 SBF differ significantly due to their initial condition when delivered, making them both promising for large-scale manufacturing of hybrid joints in building conditions. The Sikadur-370, a two-component epoxy manufactured by Sika AG, starts off as a paste-like substance and can be applied using a spatula. It has a pot life of 2.5 h and requires 8 days to fully cure at room temperature (RT). This epoxy is specifically designed for bonding steel plates to concrete for structural reinforcement, dropping the need for a primer. It is recommended to apply this adhesive with a maximum thickness of 15 mm.

On the other hand, the DuploTEC 10490 SBF, labelled DuploTEC in this manuscript, is an epoxy-based adhesive tape produced by Lohmann GmbH & Co. KG. The adhesive tape measures 0.1 mm in thickness and is covered with a polyester film. It is stored in a frozen state and can be simply laminated onto the steel substrate after thawing. When heat is applied, the tape liquefies before curing. There are two curing options: either at 130 °C for 30 min or at 170 °C for 10 min. Within this study the first curing condition is prioritized, which involves oven curing. However, for large-scale applications, induction heating, heat lamps, or other methods can be used as alternatives.

Both adhesives are qualified regarding structural and thermo-mechanical characteristics. Firstly, tensile strength and Young's modulus were determined in accordance with EN DIN 527 [29] at room temperature with a quasi-static load rate of 1 mm/min. The specimen thickness was 3 mm for Sikadur-370 and 0.1 mm for DuploTEC; results are based on the mean value of 5 samples. Secondly, lap shear strength has been performed on blasted S355 with a thickness of 3 mm in accordance with DIN EN 1465 [30] at a load rate of 5 mm/min at room temperature. Thirdly, thick adherend shear tests (TAST) specimens were manufactured and tested according to DIN EN 14869–2 [31] carried out at room temperature with a load rate 0.5 mm/min, and 5 repetitions. Additionally, glass transition temperature (T_g) is initially carried out on bulk samples after curing for at least 10 days at room temperature. The determination was carried out using dynamic mechanical analysis (DMA) in a temperature range from –20 °C to 200 °C and a heating rate of 2 K/min.

2.1.2. Grouts

Two different grout materials were used as part of the project, with one material being widely used in offshore structures, the other exhibiting a high flexural strength. The first material examined was the Densit Ducorit S8 grout material from ITW Polymers, which was certified for offshore applications (DNV-GL-ST-C502 [32]) and had been extensively tested. The second material was the high-strength grout mortar HF10 from the company Pagel, which exhibited a particularly high flexural

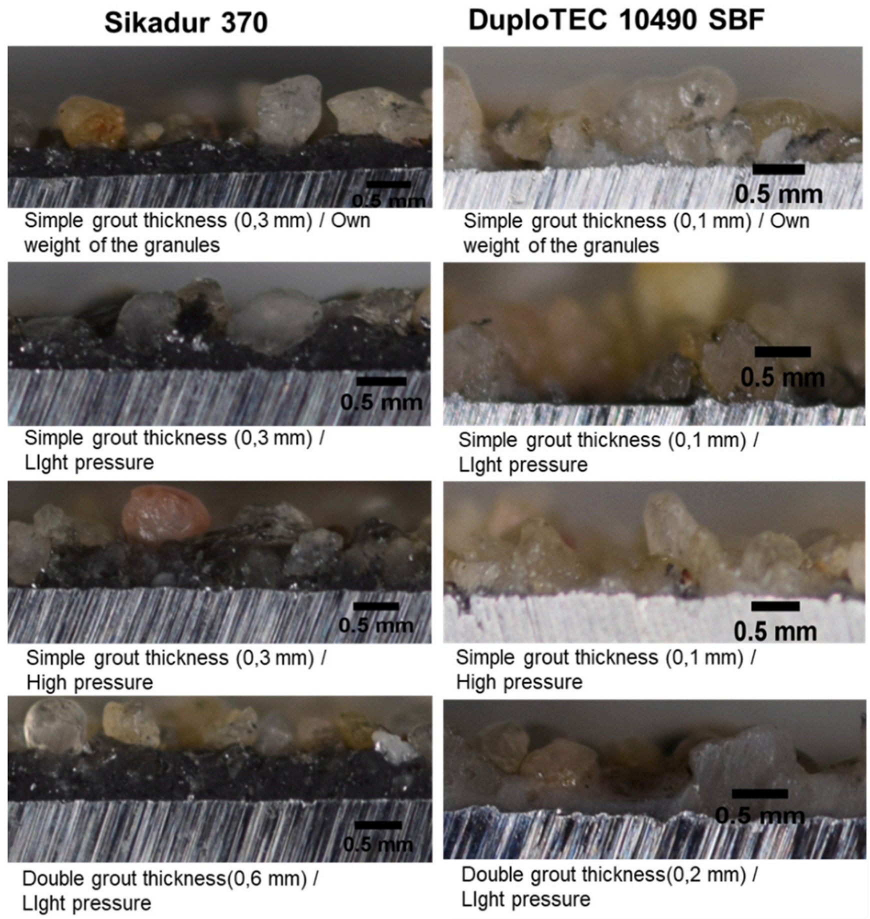

Fig. 3. Close-up of cross-sections with different adhesives, adhesive thicknesses and application pressures of the granules.

strength.

Grout material testing is done according to DIN EN 196–1 [33] using prism-shaped specimens measuring 40 mm x 40 mm x 160 mm. The bending strength is measured using a three-point bending test setup with a constant load increase rate of 50 ± 10 N/s until the specimen breaks. The results are reported as the arithmetic mean of individual results, and both individual results and the mean value should be reported to within 0.1 MPa. The compressive strength is then tested on the two halves of the specimen at a loading rate of 2400 ± 200 N/s.

2.1.3. *Granules and steel*

The goal is to enhance the mechanical interlocking mechanism by integrating particles into the adhesive. For effective embedding of the particles in the adhesive and extending into the grout layer, it is important that the particles have a sufficiently large size. Quartz sand, a commonly used filler in adhesives and grout, was identified for this purpose. To meet the geometrical requirements, a composition with a medium grain size of 1.0 mm and a narrow grain size distribution was chosen. This uniformity ensures minimal variation from the average particle size, promoting tight and even particle fit within the adhesive. This leads to improved mechanical interlocking and a more consistent and predictable performance. However, no additional specific properties of the granules or particles will be determined beyond their size and distribution.

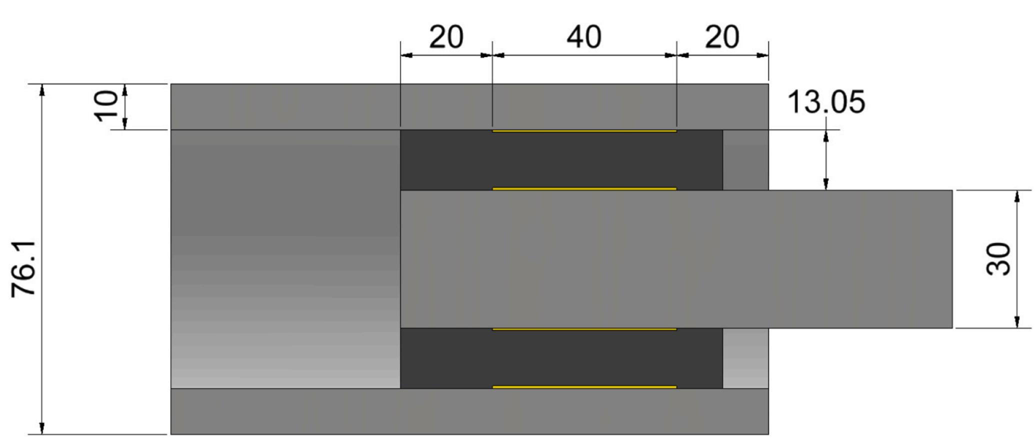

Fig. 4. Geometry of the small-scale hybrid grout joint; the adhesive layer is depicted as yellow area.

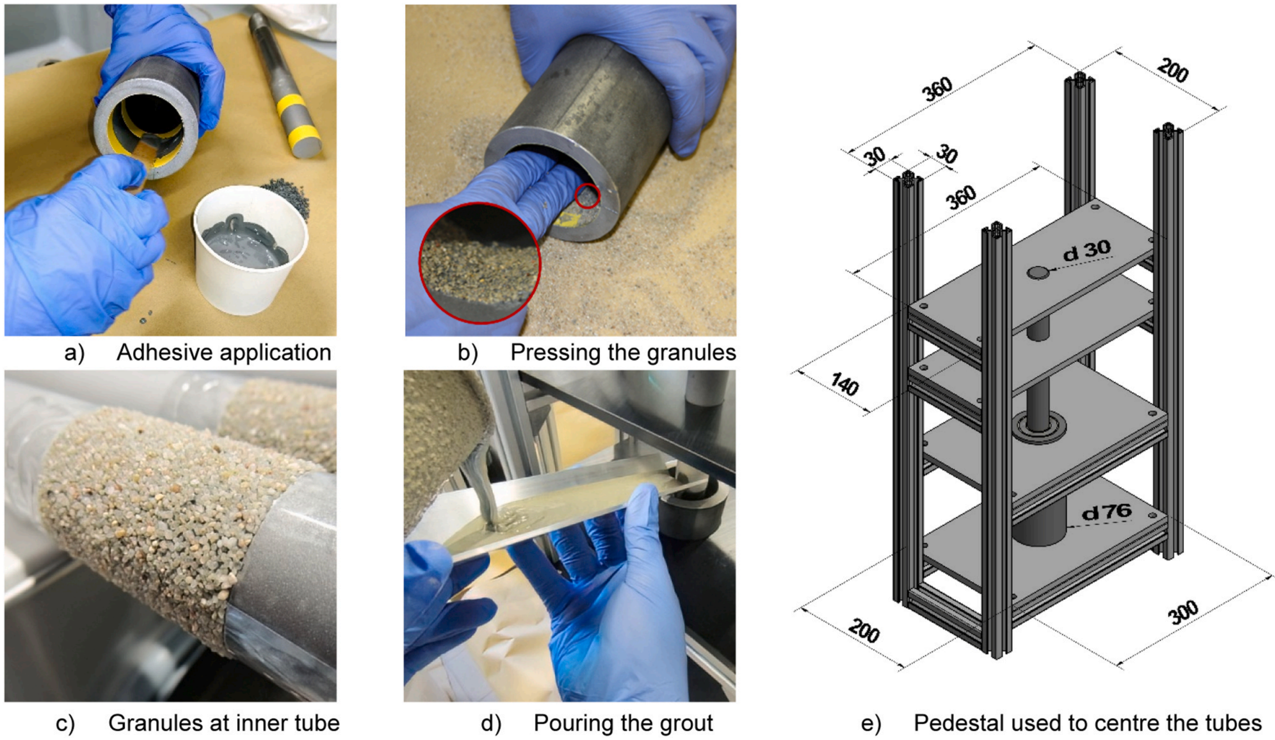

Fig. 5. Selected steps in the manufacturing of the samples.

Hot rolled circular hollow sections (CHS) manufactured in accordance with EN 10025–1 [34] from S355J2H were utilized in the study. Material properties of the steel are assumed from literature, and no specific characterisation will be performed. Additional details concerning the geometrical specifications, such as diameters and thicknesses, are provided in the following sections.

2.1.4. Composition of the adhesive-granule layer

To achieve optimal adhesive layer thickness and contact pressure, a study was undertaken on flat steel substrate surfaces, employing thin-film adhesive layers integrated with granules and quartz sand as granules. Subsequently, cross-sectional analyses were performed for each adhesive system, and the resulting data was illustrated in Fig. 3. The first row of cross sections depicted a simple adhesive layer thickness, wherein the quartz sand was spread without any pressure (Own weight of granules), leading to inadequate bonding of the grains to the adhesive. The second row displayed cross sections with a simple layer thickness, where the grains were slightly pressed (Light pressure), resulting in a desirable bonding of the granules to the adhesive for Sikadur-370, while DuploTEC exhibited a lower embedding depth due to its reduced adhesive layer thickness. The third row exhibited cross sections with strong contact pressure at a simple layer thickness, which pushed the grains down to the substrate (High Pressure) and resulted in smaller grains being fully pressed into the adhesive and surrounded by it. The fourth row displays cross sections, where a double adhesive layer thickness and light pressure were applied. Based on the favourable bonding of the granules to the adhesive, the optimal combination of a simple layer thickness and slight contact pressure was identified as the most promising approach for further investigations. Notably, the production of two adhesive tapes superimposed on each other to create double adhesive layer thickness was observed to be a convoluted and error-prone process.

2.2. Methods

2.2.1. Geometry of the hybrid joints

The hybrid grouted connections consisted of a tube-in-tube overlap joints. The sample geometry was designed to provide a sufficiently large gap for grout filling, while ensuring an estimated failure load below 150 kN (the maximum load of the specific UTM used). The (outer) sleeve had a diameter of 76.1 mm and a thickness of 10 mm, while the (inner) pile was a solid steel rod with a diameter of 30 mm; this resulted in a nominal gap of 13.05 mm. The adhesive layer had a 40 mm overlapping length. Polyethylene adhesive tape was applied above and below the adhesive layer to prevent grout material bonding to the joint components. The total sample length was 505.5 mm. Tests were performed in a UTM at a displacement rate of 0.5 mm/min.

2.3. Manufacturing procedure for the hybrid joints

The manufacturing process of the hybrid grouted joint involved different steps, illustrated by Fig. 5. Prior to the application of the adhesive, surface preparation of the steel was carried out by blasting with corundum to Sa 2 ½ level and degreasing with butanone (also known as methyl ethyl ketone, MEK). A 0.5 mm textile tape was used to define the lateral boundaries and thickness of the adhesive layers. After curing, the tape was removed, and quartz sand was spread on the wet adhesive, which was subsequently pressed onto the steel surface. The curing process was conducted according to the manufacturer's guidelines. The adherends were then grouted in an upright position, and a fixture was used to ensure correct alignment. To set the overlap length, the inner CHS was placed on a circular pedestal, which could be positioned inside the outer CHS at a defined height via a threaded rod. This pedestal also served as the bottom seal of the grout layer. The grout was mixed following the manufacturer's instructions and poured directly into the gap. The self-levelling and self-compacting properties of the grout ensured sufficient filling of the gap. To prevent shrinkage, the surface of the grout layer was kept moist and sealed with a polyethylene film for 28 days during the curing period.

Fig. 6. (left) Hinge at the bottom of the sample, (right) the pair of LVDT measuring the relative displacement.

2.4. Mechanical testing

Tensile tests were conducted using universal testing machines and specific testing rigs were used. They were clamped onto fork sockets with bolts offset by 90° to allow for full rotation, comparable to a clevis head; Fig. 6-a show the lower part of the test setup. All tests used displacement control. Load and machine displacement were measured. Additionally, linear Variable Differential Transformers (LVDT) were used to monitor relative displacement between the CHS, depicted in Fig. 6-b.

2.5. Experimental series

2.5.1. Tests under laboratory conditions

Two adhesives, Sikadur-370 and DuploTEC, were used along with two grout materials, Pagel HF10 and Ducorit S8, and quartz sand as the aggregate. This resulted in four configurations, which were tested five-fold, thus a total of 20 individual tests. Manufacturing, curing, and storing were performed under laboratory conditions, which are 23 °C and 50% rel. humidity, on samples not subjected to any ageing procedure—subsequently labelled as reference.

2.5.2. Tests under low and elevated temperatures

The hybrid grouted connection is planned to find application in steel high-rise and bridge construction and in the offshore sector. To assess the influence of high and low temperatures on the load-bearing behaviour of the hybrid grout connection, tensile tests were conducted at + 60 °C and –20 °C; the choice of these temperature being based upon investigations summarised in an earlier publication set up in the same North-Sea and Baltic setting [6]. Twenty quasi-static tensile tests were performed on a servo-hydraulic testing machine at a displacement rate of 0.5 mm/min; tests were performed in a climatic chamber.

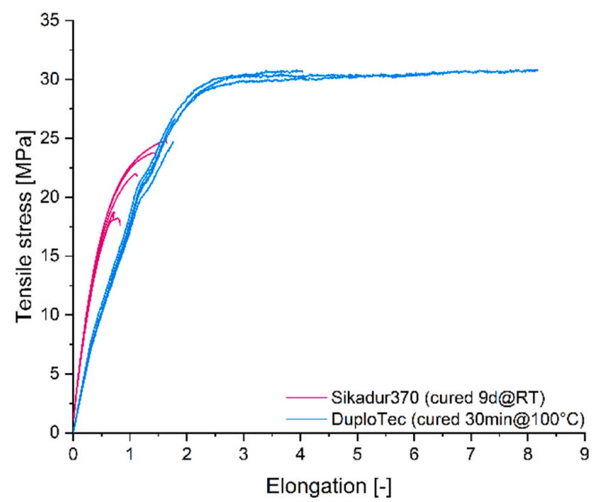

Fig. 8. Results of the tensile tests.

2.5.3. Ageing tests

The assessment of long-term durability in bonded connections often includes subjecting them to artificial ageing under harsh environmental conditions. This involves comparing key parameters, such as load-

Fig. 7. Samples during the ageing tests.

Table 1
Mechanical properties of the adhesives.

Adhesive	DMA	Adhesive Bulk			Lap shear	TAST (thick adherend shear tests)		
	T_G in °C	σ_{max} in MPa	ε_{max} in %	E in MPa	τ_{max} in MPa	τ_{max} in MPa	γ_{max}	G in MPa
Sikadur-370	75,74	21,5 ± 2,9	1,1 ± 0,4	3‘581 ± 113	27,50 ± 1,16	27,26 ± 6,04	0,1—0,2	882 ± 477
DuploTEC 10490 SBF	139,50	28,7 ± 2,9	4,1 ± 2,8	1593 ± 44	27,39 ± 1,12	45,91 ± 6,29	1—3	210 ± 54

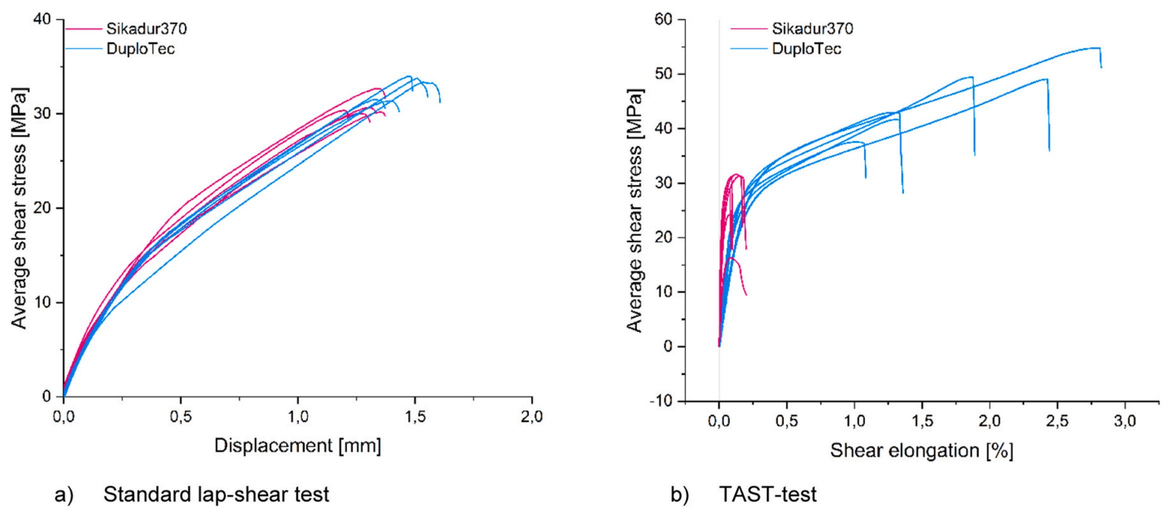

Fig. 9. Results of the shear tests.

bearing capacity after aging, with reference values obtained from the unaged state. In this study, ageing was performed using two methods: water immersion in accordance with DIN EN ISO 15711:2004 [35], and a climate change test based on VW-PV1200 as described in [36].

The water immersion test consisted of exposing the samples to artificial seawater for 1′000 h. The artificial seawater was prepared according to DIN EN ISO 15711:2004 [47] with a composition of 23 g/ℓ NaCl, 9.8 g/ℓ, $MgCl_2$, 8.9 g/ℓ, Na_2SO_4, and 1.2 g/ℓ $CaCl_2$. For each test series, five samples were placed in containers, ensuring full submersion of the hybrid grouted connection while keeping the threaded ends positioned above the waterline to prevent corrosion, as shown in Fig. 7-a. The containers containing the samples were stored in laboratory conditions throughout the 1′000-hour immersion period. Following the immersion, tests were conducted to assess the remaining load-bearing capacity using the protocol outlined in section 3.3.

The climatic cycling test, following the VW PV 1200 [36] standard, involved cyclic variations of temperature and humidity. To simulate the intended operating conditions of hybrid grouted connections in steel construction, temperature ranges were limited to + 60 °C for high temperature (at 90% relative humidity) and –20 °C for low temperature, all this in the climatic chamber shown in Fig. 7-b. Each cycle lasted 12 h, and the test was run for a total of 70 cycles, resulting in a 35-day accelerated ageing process. Testing of the residual load capacity was carried out using the protocol outlined in section 3.3.

3. Results

3.1. Material characterisation

3.1.1. Adhesives: tensile tests

In the tests of this series, the specimens were subjected to quasi-static loading at room temperature with a traverse speed of 1 mm/min. Local deformation of the samples was measured using external displacement sensors. The results were based on the average of 5 samples. Sikadur-370

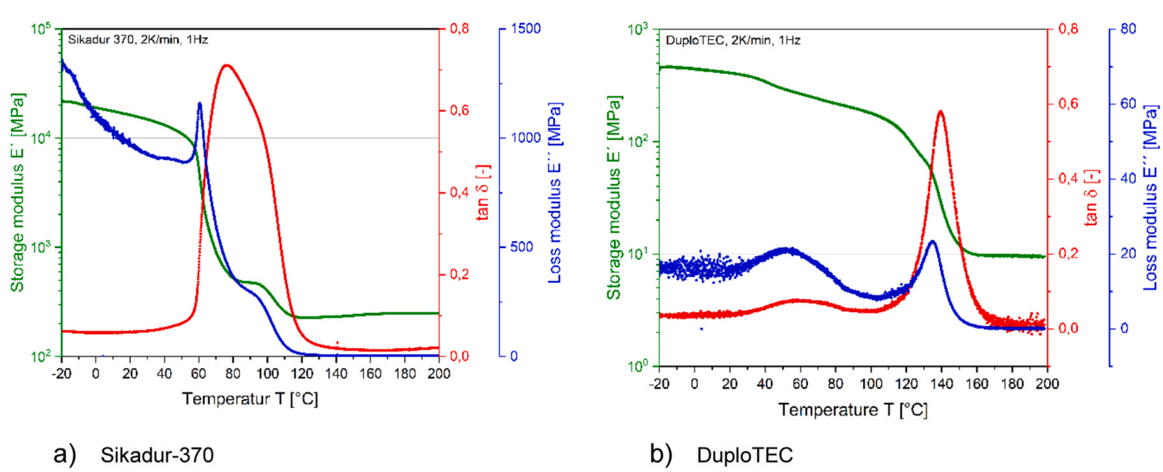

Fig. 10. Results of the dynamic-mechanical analysis.

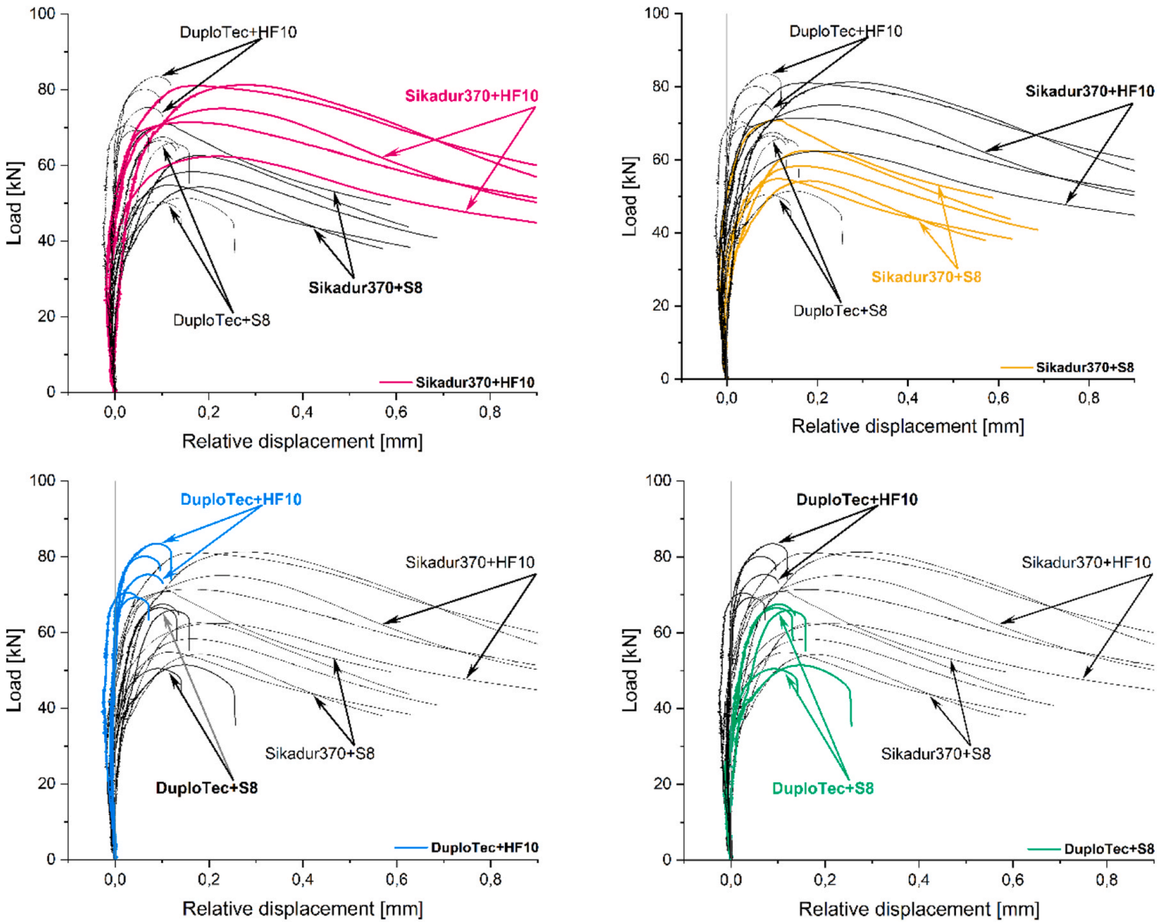

Fig. 11. Experimental results of the small-scale hybrid joints.

exhibited mostly linear elastic behaviour, and minor decreasing slope at higher stresses. On the other hand, DuploTEC showed an initial linear increase followed by a steady plateau at around 30 MPa. The elasticity modulus, listed in Table 1, was determined within the linear range of small deformations; both adhesives met the specified functional limits for stiffness.

3.1.2. Adhesives: shear tests

Quasi-static tensile shear tests were conducted on blasted S355 steel sheets, adhering to DIN EN 1465 standards, at room temperature. The force-displacement curves for both adhesives exhibited similar patterns, as shown in Fig. 9-a. Initially, there was a linear increase in force up to approximately 15 to 18 MPa. Following this, the slope gradually decreased. In both cases, the lap shear strength reached an approximate value of 32 MPa, with cohesive failure. All derived results are listed in Table 1.

Additionally, thick adherend shear tests (TAST) allowed the determination of the shear modulus G, with a comprehensive summary of all the results to be found in Table 1. In these tests, both shear-elongation to shear stress curves shown in Fig. 9-b were bi-linear, with DuploTEC

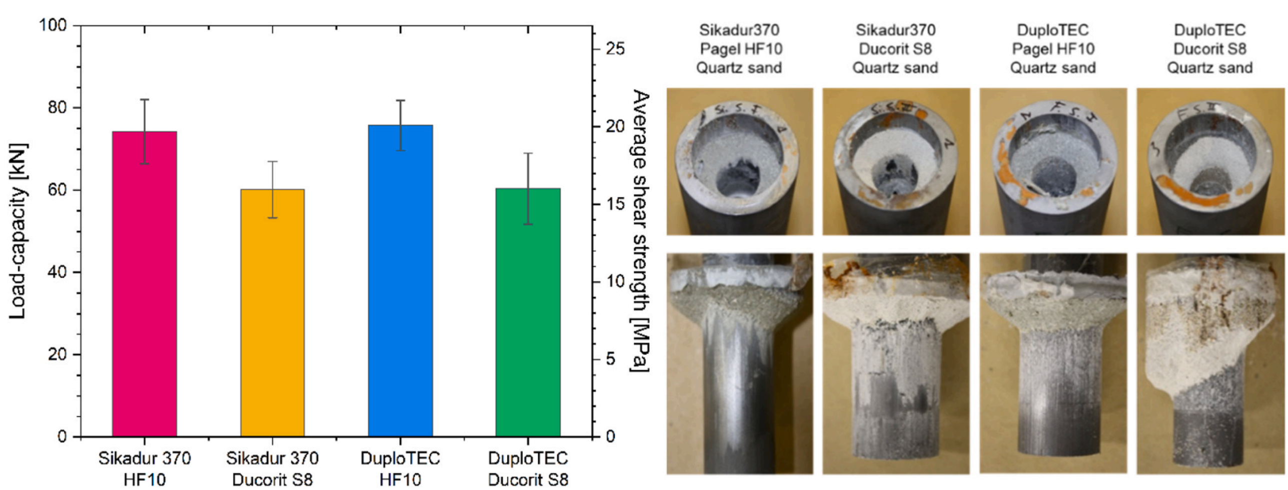

Fig. 12. (left) Load-capacities and (right) representative fracture patterns of the reference hybrid grout joints.

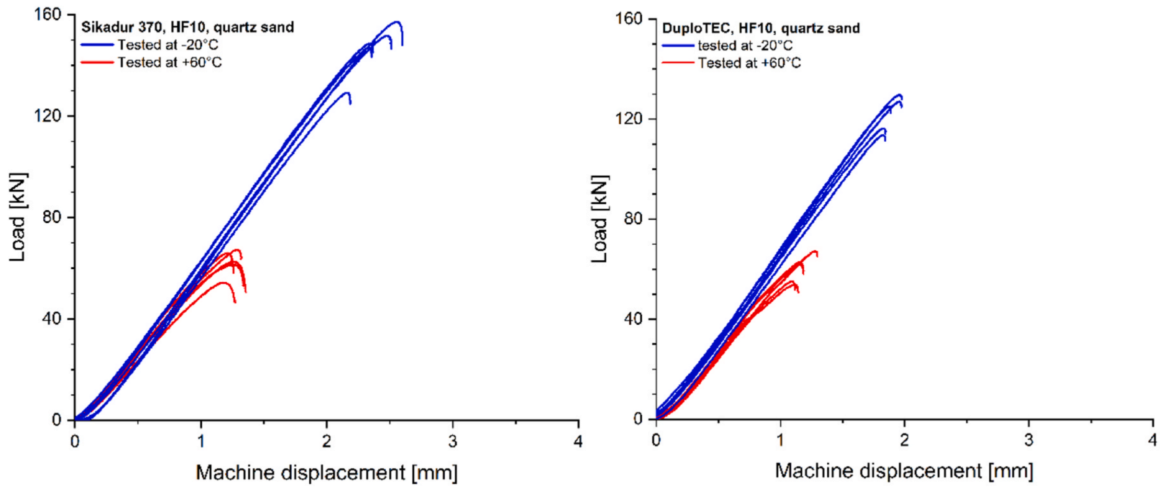

Fig. 13. Experimental results of the small-scale hybrid joints tested at T = −20 °C and T = 60 °C.

demonstrating a more pronounced behaviour. DuploTEC's bilinear pattern displayed a distinct kink at approximately 0.17 shear elongation (around 29.5 MPa shear stress), beyond which the shear stiffness decreased significantly. On the other hand, Sikadur-370 reached a peak shear strength of approximately 32 MPa (excluding one outlier), while DuploTEC achieved even higher values of around 50 MPa (albeit with slightly greater variability). Regarding maximum elongation, Sikadur-370 measured between 0.1% and 0.2%, whereas DuploTEC exhibited a range of 1 to 3%.

3.1.3. Adhesives: dynamic-mechanical analysis, DMA

Determination of the glass transition temperature T_g was performed on adhesive samples cured for 10 days at room temperature. The results are presented in Fig. 10. Sikadur-370 exhibited a T_g of 75.5 °C, considering the loss factor tanδ; however, its elastic modulus showed a significant decrease after 60 °C. DuploTEC displayed a higher T_g of 139.5 °C, with a noticeable decrease in the elastic modulus starting only after 100 °C. Both Sikadur-370 and DuploTEC 10490 SBF clearly met the $T_g > 67$ °C criterion.

3.1.4. Characterisation of the grouts

Six prisms are manufactured and tested per grout material. Both materials exhibit high strengths, with the compressive strength of HF10 to 123.4 ± 2.6 MPa, and that of Ducorit S8 to 104.1 ± 3.1 MPa. The flexural strength of HF10, 17.9 ± 1.4 MPa, was much higher than that of S8, 10.7 ± 0.5 MPa. Both materials show very small scatter in strength, with coefficients of variation between 2% and 7%.

3.2. Tensile tests on small-scale hybrid joints

3.2.1. Tests under laboratory conditions

The experimental load capacities of the small-scale hybrid grouted joints using Sikadur-370 and DuploTEC adhesives, along with Pagel HF10 and Ducorit S8 grout materials, with quartz sand are shown in Fig. 12. Among these combinations, the highest load capacities are achieved by Sikadur-370 (74.2 kN) and DuploTEC (75.7 kN) in combination with Pagel HF10. In comparison, the load capacities of all adhesives combined with Ducorit S8 as the grout material are approximately 20% lower than those with Pagel HF10, which aligns with the relative difference in compressive strengths between the two grout materials.

In addition to the load capacities, the fracture patterns of the small-scale hybrid test specimens were also scrutinised. Representative fracture patterns for each parameter combination are shown in Fig. 12. The fracture patterns are similar in all specimens, with a cone-shaped fracture zone formed by grout material on the (inner) pile at the upper overlap end. Below the fracture cone, adhesive and cohesive failure can be seen towards the pile.

3.2.2. Tests under low and elevated temperatures

Based on the results of the tests at laboratory conditions the prioritized grout material used in all test series was Pagel HF10. Therefore, the parameter variation solely pertained to the adhesive system. In general, the tensile strength and stiffness of cured adhesives decrease with increasing temperature. However, all other materials involved in the hybrid grout connection (steel, grout, and quartz sand) exhibit much less sensitivity to temperature. The resulting load-displacement curves can be seen in Fig. 13.

As these tests were carried out in a temperature chamber, the displacement is measured by the traverse movemenet of the machine. The load-displacement curves show that the stiffness is similar at T = −20 °C and T = 60 °C. The stiffness at RT is assumed to be the same, but as these tests were carried out on a different machine, the load-displacement curves are not comparable.

Fig. 16 provides a summary of the load-bearing capacities F_{max}. For the hybrid joints involving Sikadur-370, the average load-bearing capacity at –20 °C, with $F_{max} = 146.8$ kN, is almost twice as high as at room temperature. However, at a temperature of 60 °C, a reduction of a mere 20% in load-bearing capacity is reported, if compared to the load-bearing capacity at room temperature. For the DuploTEC adhesive system, it can be observed that the average load-bearing capacity at –20 °C, with 122.4 kN, is approximately 60% higher than the average load-bearing capacity at room temperature. At + 60 °C, the average load-bearing capacity, 60.1 kN, is approximately 20% lower than that at room temperature.

As expected, a low temperature can be considered non-critical in terms of load-bearing capacity, as validated by the significant increases in load-bearing capacities. However, from an application point of view, the minimal reduction in load-bearing capacity of approximately 20% at the application temperature of 60 °C should also be considered positive. Furthermore, it should be noted that the scatter of test results at high and low temperatures does not change significantly, remaining within a range of up to a maximum of approximately 10 kN.

In addition to load-bearing capacity, fracture surfaces were also analysed. In Fig. 14, a representative fracture surface is shown for each adhesive system and each tested temperature. For samples bonded with Sikadur-370, cohesive failure is observed below the fracture cone on the inner rod at –20 °C, while at room temperature, it is less prominent. Only adhesive failure occurs at elevated temperatures. DuploTEC bonded samples show no significant changes in the fracture pattern due

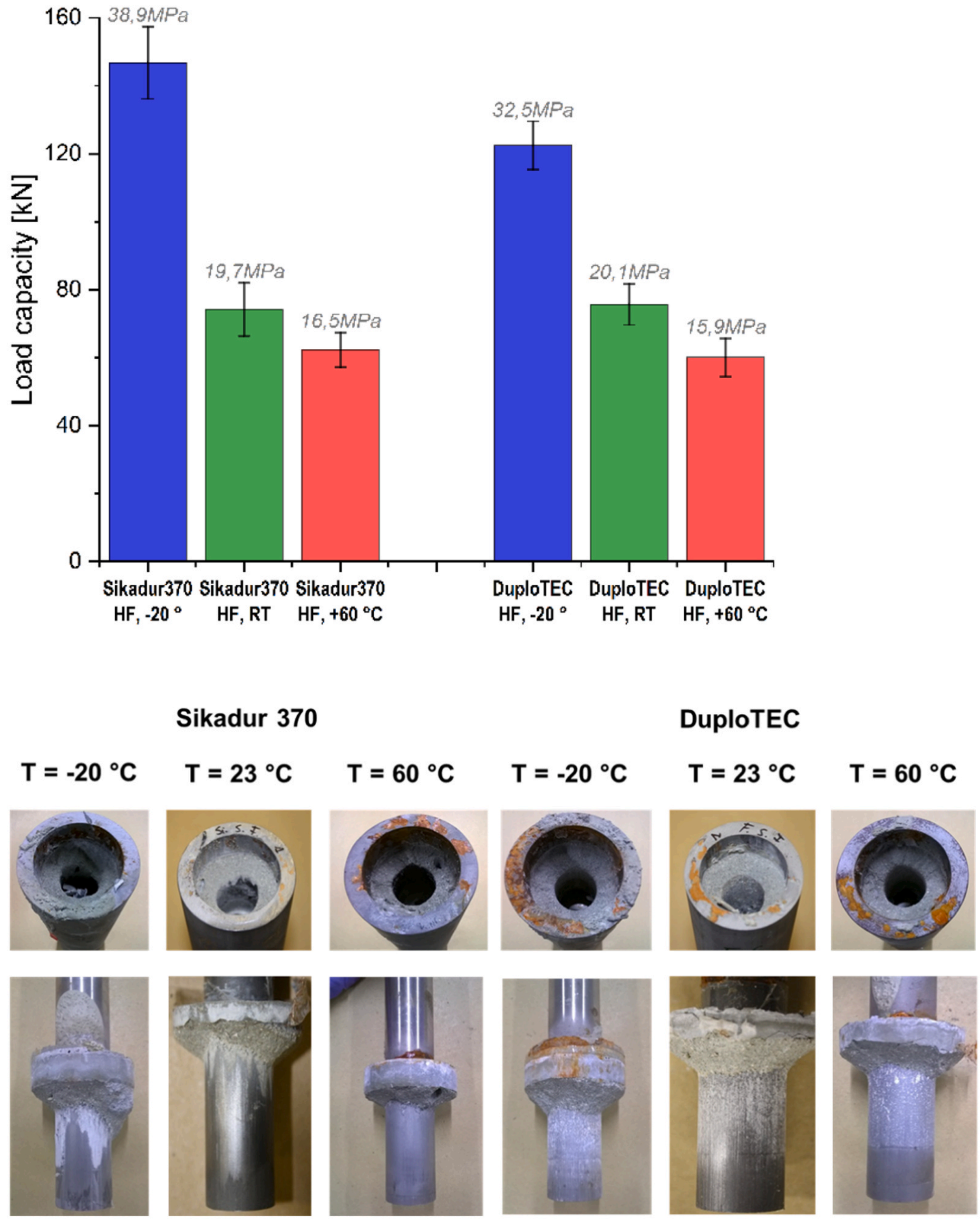

Fig. 14. (top) Load-capacities and (bottom) representative fracture patterns of the hybrid grout joints, at low, normal, and elevated temperatures.

to temperature variations.

3.2.3. *Ageing tests*

After the artificial seawater exposure, significant corrosion is visible, accompanied by a brownish discoloration of the seawater; cf. Fig. 7-a. The specimens subjected to the climatic cycling test also show corrosion marks, shown in Fig. 7-b, although the corrosion layer is less pronounced compared to the artificial seawater exposure.

Fig. 15 shows the load-displacement curves after the immersion in artificial sea-water and climatic changing.

The load capacities of samples subjected to exposure in artificial seawater and climatic cycling tests are summarized in Fig. 16, including the corresponding unaged reference value. As shows Fig. 16 (up), the load-bearing capacity of samples bonded with Sikadur-370 increases by (on average) approximately 34 kN in the climatic cycling test, if compared to the (averaged) unaged reference value. The load-bearing capacity after exposure to artificial seawater is also higher than in the unaged state, with an increase of only about 21 kN. One possible explanation for this unexpected increase in load-bearing capacity is that the adhesive system Sikadur-370 may undergo further curing during the exposure period. No significant change in load-bearing capacity is observed for samples involving DuploTEC due to exposure.

Fig. 16 (bottom) illustrates the effects of exposure to artificial seawater and the climatic cycling test on the specimens: fracture surfaces were examined for each adhesive and exposure condition. For DuploTEC, corrosion marks are observed at the upper end of the fracture cone after water exposure. This area had a polyethylene strip (by Tesa) inserted between the grout and the outer pipe to prevent bonding, and it seems that water penetration caused the corrosion marks. The same observation applies to the other exposed specimens. However, no corrosion infiltration is noticeable in the adhesive failure area at the inner tube for any of the samples. In conclusion, both adhesive systems effectively protect the metallic joint surfaces from corrosion. All results of the quasi-static tensile tests on the small-scale hybrid specimens

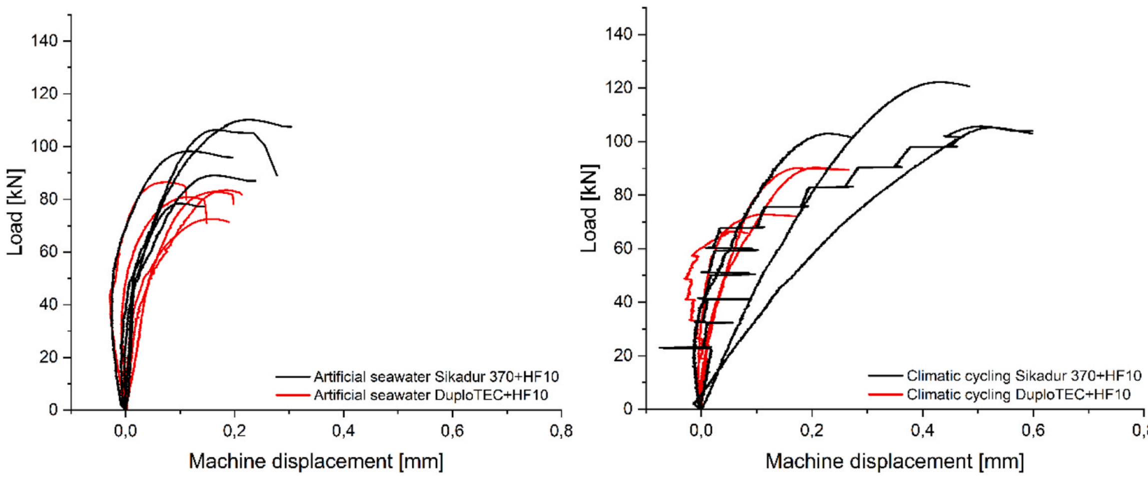

Fig. 15. Experimental results of the small-scale hybrid joints tested after immersion in (left) artificial seawater and ageing by (right) climatic cycling.

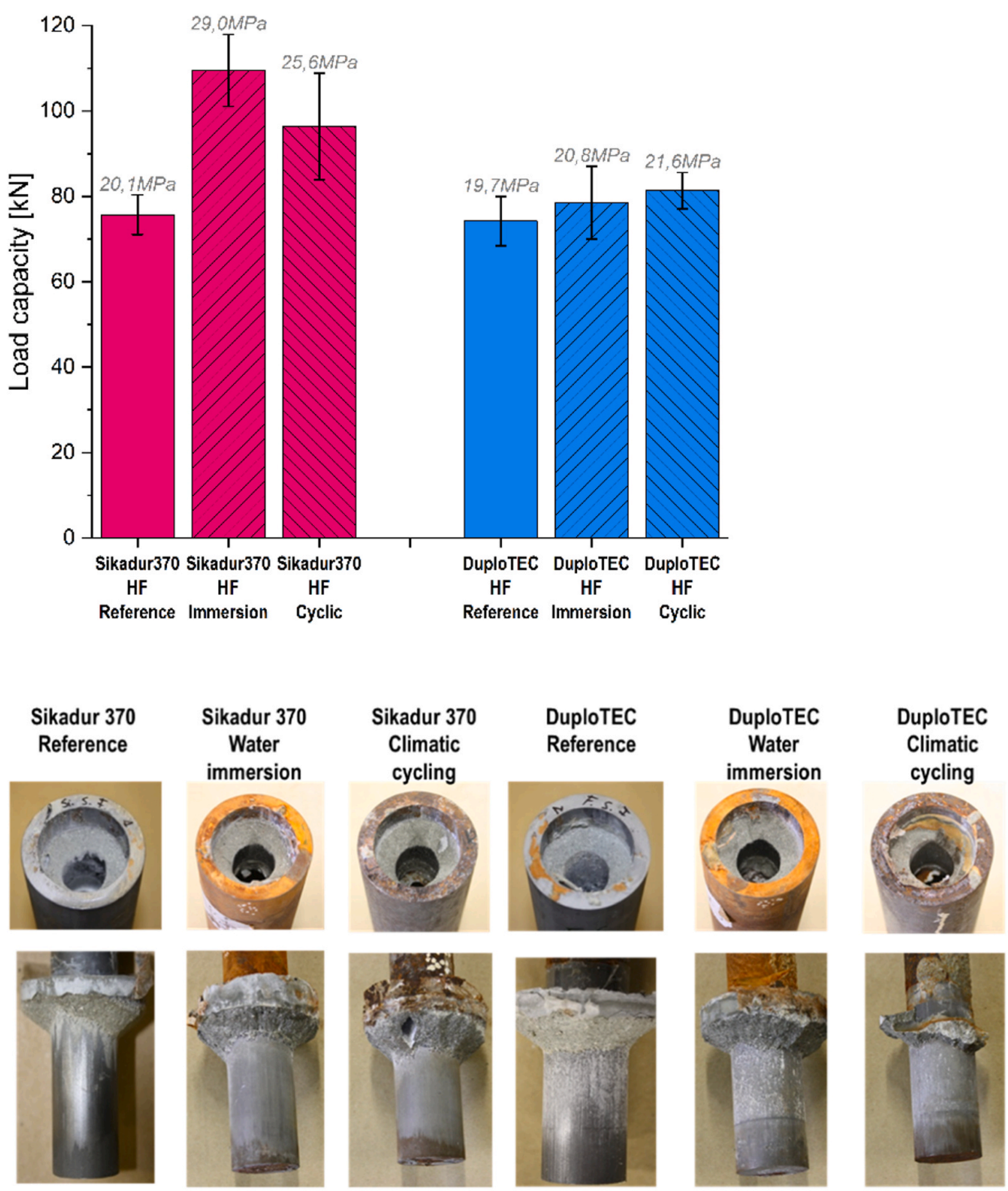

Fig. 16. (top) Load capacities of aged hybrid joints, compared to the reference, (bottom) failure modes of the aged hybrid joints.

Table 2
Load capacities of small-scale hybrid specimens.

Adhesive/ Grout combination	Temperature						Durability			
	RT (reference)		T = −20 °C		T = 60 °C		water immersion		climate change	
	F_{max} in kN	σ_{max} in MPa	F_{max} in kN	σ_{max} in MPa	F_{max} in kN	σ_{max} in MPa	F_{max} in kN	σ_{max} in MPa	F_{max} in kN	σ_{max} in MPa
Sikadur-370/ HF10	74,2 ± 7,8	19,7 ± 2,1	122,4 ± 7,1	32,5 ± 1,9	60,1 ± 5,6	15,9 ± 1,5	96,4 ± 12,9	29,0 ± 3,4	109,5 ± 7,7	25,6 ± 2,0
Sikadur-370/ Ducorit S8	60,2 ± 6,8	16,0 ± 1,8	/	/	/	/	/	/	/	/
DuploTEC 10490 SBF/ HF10	75,7 ± 6,1	20,1 ± 1,6	146,8 ± 10,6	38,9 ± 2,8	62,3 ± 5,1	16,5 ± 1,4	81,3 ± 5,3	20,8 ± 1,4	78,5 ± 10,9	21,6 ± 2,9
DuploTEC 10490 SBF/ Ducorit S8	60,4 ± 8,6	16,0 ± 2,3	/	/	/	/	/	/	/	/

are summarised in Table 2.

In summary, the hybrid grout connections exhibit high resistance to external influences, as evidenced by the absence of corrosion infiltration in the joint area and, in the case of Sikadur-370, a significant increase in residual load-bearing capacity compared to the unaged state.

4. Discussion and conclusions

The study investigated the load bearing capacities and fracture patterns of small-scale hybrid test specimens. Before manufacturing hybrid grouted specimens, an initial study regarding the optimal adhesive thickness-granules combination was conducted. Cross-sectional analyses showed, that quartz sand with a single adhesive layer thickness (0.5 mm for liquid adhesive or 0.1 mm for adhesive tape) is optimal.

The fracture patterns of the hybrid grouted specimens generally featured a cone-shaped zone formed by grout material on the inner tube at the upper overlap end, with adhesive and cohesive failure observed below. The parameter combinations with the highest load capacities in combination with quartz sand were prioritized for further experiments: a) Sikadur-370, Pagel HF10, and quartz sand, and b) DuploTEC, Pagel HF10, and quartz sand.

Temperature had a different effect on load-bearing capacities, depending on the adhesive. For the Sikadur-370 adhesive system, load-bearing capacity at − 20 °C was nearly double that at room temperature, while at 60 °C, there was a reduction of about 20%. For the DuploTEC adhesive system, load-bearing capacity at − 20 °C was approximately 60% higher than at room temperature, and at 60 °C, there was a reduction of about 20%. Overall, low temperatures had a positive impact on load-bearing capacity, while the reduction at high temperatures remained within an acceptable range for practical applications.

Fracture patterns did not exhibit significant changes due to temperature variations in DuploTEC samples, while cohesive failure occurred below the fracture cone on the inner tube in Sikadur-370 samples at –20 °C, with adhesive failure at elevated temperatures.

The study also evaluated the effects of exposure to artificial seawater and climatic cycling tests. Samples bonded with Sikadur-370 showed an increase in load-bearing capacity after the climatic cycling test and exposure to artificial seawater, suggesting further crosslinking of the adhesive system. No significant change in load-bearing capacity was observed in DuploTEC samples due to exposure. Corrosion signs were visible in specimens exposed to artificial seawater and the climatic cycling test, but both adhesive systems effectively protected the metallic joint surfaces from corrosion.

In conclusion, the hybrid grout connection method presented in this research offers advantages over traditional joining methods for steel components. Extensive investigations were conducted to analyse the mechanical properties and performance of the hybrid connection. Suitable materials were selected and characterized, and tests were performed to evaluate their properties. The constructive design and manufacturing processes were optimized based on these findings. Tensile tests on hybrid grouted tube connections helped identify efficient combinations of adhesive, grout material, and granulate.

Overall, the hybrid grouted connections demonstrated improved load-bearing capacities when exposed to artificial seawater and climatic cycling tests. Sikadur-370-bonded samples showed a significant increase in load-bearing capacity, potentially due to further crosslinking during exposure. DuploTEC-bonded samples showed no significant change in load-bearing capacity. Both adhesive systems effectively protected the joint surfaces from corrosion. These findings highlight the potential of hybrid grout connections as a reliable alternative for joining steel components in various applications.

CRediT authorship contribution statement

Sebastian Myslicki: Supervision, Project administration, Conceptualization, Methodology, Validation, Formal analysis, Investigation, Data Curation, Writing - Original Draft, Writing - Review & Editing, Visualization. Till Vallée: Writing - Original Draft, Visualization, Data Curation. Holger Fricke: Resources, Funding acquisition, Methodology. Thomas Ummenhofer: Resources, Supervision, Funding acquisition. Jakob Boretzki: Writing - Original Draft, Visualization, Project administration, Visualization, Formal analysis. Matthias Albiez: Writing - Review & Editing, Project administration, Funding acquisition.

Declaration of Competing Interest

The authors declare the following financial interests/personal relationships which may be considered as potential competing interests: Sebastian Myslicki, Till Vallée, Holger Fricke, Thomas Ummenhofer, Jakob Boretzki and Matthias Albiez reports financial support was provided by German Federation of Industrial Research Associations. Thomas Ummenhofer and Matthias Albiez has patent ###EP3237765B1 issued to Karlsruher Institut fuer Technologie KIT.

Data availability

Data will be made available on request.

Acknowledgements

This research was supported by the German Federal Ministry of Economic Affairs and Climate Action through the German Federation of Industrial Research Associations (AiF) as part of the program for promoting industrial cooperative research (project IGF 19989 N of the Research Association for Steel Application – FOSTA).

References

[1] N.W. Krahl, D.I. Karsan, Axial strength of grouted pile-to-sleeve connections, J. Struct. Eng. 111 (4) (1985) 889–905, https://doi.org/10.1061/(ASCE)0733-9445(1985)111:4(889).
[2] C. Denkert, T. Gerke, R. Glienke, M. Dörre, M.K. Henkel, H. Fricke, et al., Experimental investigations on pre-tensioned hybrid joints for structural steel

applications, J. Adhes. 99 (2) (2023) 117–152, https://doi.org/10.1080/00218464.2021.2003786.
[3] M. Albiez, J. Damm, T. Ummenhofer, M. Kaufmann, T. Vallée, S. Myslicki, Hybrid joining of jacket structures for offshore wind turbines – Determination of requirements and adhesive characterisation, Eng. Struct. 259 (2022) 114186, https://doi.org/10.1016/j.engstruct.2022.114186.
[4] M. Albiez, T. Vallée, T. Ummenhofer, Adhesively bonded steel tubes – Part II: numerical modelling and strength prediction, Int. J. Adhes. Adhes. 90 (2019) 211–224, https://doi.org/10.1016/j.ijadhadh.2018.02.004.
[5] M. Albiez, T. Vallée, T. Ummenhofer, Adhesively bonded steel tubes - Part II: numerical modelling and strength prediction, Int. J. Adhes. Adhes. 90 (2019) 211–224, https://doi.org/10.1016/j.ijadhadh.2018.02.004.
[6] M. Albiez, J. Damm, T. Ummenhofer, M. Kaufmann, T. Vallée, S. Myslicki, Hybrid joining of jacket structures for offshore wind turbines - Determination of requirements and adhesive characterisation, Eng. Struct. 259 (2022) 114186, https://doi.org/10.1016/j.engstruct.2022.114186.
[7] Da Silva L.F.M. Design Rules and Methods to Improve Joint Strength. In: Da Silva LFM, Öchsner A, Adams RD, editors. Handbook of Adhesion Technology. Berlin, Heidelberg: Springer Berlin Heidelberg; 2011, p. 689–723.
[8] N.I. Tziavos, H. Hemida, N. Metje, C. Baniotopoulos, Grouted connections on offshore wind turbines: a review, Proc. Inst. Civ. Eng. Eng. Comput. Mech. 169 (4) (2016) 183–195, https://doi.org/10.1680/jencm.16.00004.
[9] P. Dallyn, A. El-Hamalawi, A. Palmeri, R. Knight, Experimental testing of grouted connections for offshore substructures: a critical review, Structures 3 (2015) 90–108, https://doi.org/10.1016/j.istruc.2015.03.005.
[10] G. Solland, A. Johansen, Design recommendations for grouted pile sleeve connections, Mar. Struct. 60 (2018) 1–14, https://doi.org/10.1016/j.marstruc.2018.03.001.
[11] Schaumann P., Wilke F. Design of Large Diameter Hybrid Connections Grouted With High Performance Concrete. The Seventeenth International Offshore and Polar Engineering Conference 2007.
[12] Klose M., Faber T., Schaumann P., Lochte-Holtgreven S. Grouted Connections For Offshore Wind Turbines. The Eighteenth International Offshore and Polar Engineering Conference 2008.
[13] Schaumann P., Lochte-Holtgreven S., Eichstädt R., Camp T., McCann G. Numerical Investigations on Local Degradation and Vertical Misalignments of Grouted Joints in Monopile Foundations. The Twenty-third International Offshore and Polar Engineering Conference 2013.
[14] Till Vallée, Matthias Albiez. 17 - Building and construction steel and aluminium. In: Adams RD, editor. Adhesive bonding: Science, technology and applications. Oxford: Woodhead Publishing; 2021, p. 525–569.
[15] M. Albiez, T. Vallée, H. Fricke, T. Ummenhofer, Adhesively bonded steel tubes — Part I: experimental investigations, Int. J. Adhes. Adhes. 90 (2019) 199–210, https://doi.org/10.1016/j.ijadhadh.2018.02.005.
[16] C.H. Desch, General discussion on cohesion and related problems. Cohesion: a general survey, Trans. Faraday Soc. 24 (1928) 53–64.
[17] Younes Jahani, Marta Baena, Cristina Barris, Ricardo Perera, Lluís Torres, Influence of curing, post-curing and testing temperatures on mechanical properties of a structural adhesive, Constr. Build. Mater. 324 (2022) 126698, https://doi.org/10.1016/j.conbuildmat.2022.126698.
[18] R.D. Adams, J. Coppendale, V. Mallick, H. Al-Hamdan, The effect of temperature on the strength of adhesive joints, Int. J. Adhes. Adhes. 12 (3) (1992) 185–190, https://doi.org/10.1016/0143-7496(92)90052-W.
[19] K.W. Allen, Some reflections on contemporary views of theories of adhesion, Int. J. Adhes. Adhes. 13 (2) (1993) 67–72, https://doi.org/10.1016/0143-7496(93)90015-2.
[20] Irwin D.S., Johnson T.C. Comparison of solvents for cleaning metal surfaces. Denver, Colorado, Washington, D.C: Dow Chemical Company, Rocky Flats Plant; Office of Technical Services, Department of Commerce; 1964.
[21] M. Albiez, J. Damm, T. Ummenhofer, H. Ehard, C. Schuler, M. Kaufmann, et al., Hybrid joining of jacket structures for offshore wind turbines - Validation under static and dynamic loading at medium and large scale, Eng. Struct. 252 (2022) 113595, https://doi.org/10.1016/j.engstruct.2021.113595.
[22] K. Yokozeki, K. Hisazumi, T. Vallée, T. Evers, T. Ummenhofer, J. Boretzki, et al., Hybrid joints consisting of pre-tensioned bolts and a bonded connection, Part II: large-scale experiments, Int. J. Adhes. Adhes. (2023) 103523, https://doi.org/10.1016/j.ijadhadh.2023.103523.
[23] S. Myslicki, H. Kordy, M. Kaufmann, R. Créac`hcadec, T. Vallée, Under water glued stud bonding fasteners for offshore structures, Int. J. Adhes. Adhes. 98 (2020) 102533, https://doi.org/10.1016/j.ijadhadh.2019.102533.
[24] Adams R.D. (ed.). Adhesive bonding: Science, technology and applications. Oxford: Woodhead Publishing; 2021.
[25] L.F.M. Da Silva, A. Öchsner, R.D. Adams, Introduction to adhesive bonding technology. In: Handbook of adhesion technology, Springer, 2018, pp. 1–7.
[26] C.A. Coulomb, Theorie des machines simples, en ayant egard au frottement de leurs parties et a la roideur des cordages. Nouv, Bachelier, 1821.
[27] Y. Bai, T. Wierzbicki, Application of extended Mohr–Coulomb criterion to ductile fracture, Int. J. Fract. 161 (1) (2010) 1–20, https://doi.org/10.1007/s10704-009-9422-8.
[28] Till Vallée, Marvin Kaufmann, Robert D. Adams, Matthias Albiez, João R. Correia, Thomas Tannert, Are probabilistic methods a way to get rid of fudge factors? Part I: background and theory, Int. J. Adhes. Adhes. 119 (2022) 103255, https://doi.org/10.1016/j.ijadhadh.2022.103255.
[29] Deutsches Institut für Normung. DIN EN ISO 527–2:2012–06 Plastics - Determination of tensile properties - Part 2: Test conditions for moulding and extrusion plastics. Berlin: Beuth Verlag GmbH. https://doi.org/10.31030/1860304.
[30] DIN EN ISO 1465:2009–07. Adhesives - Determination of tensile lap-shear strength of bonded assemblies. Berlin: Beuth; 2009; Available from: 〈http://www.beuth.de/de/norm/din-en-1465/115724482〉.
[31] Deutsches Institut für Normung. 14869–2: 2011-07. Structural adhesives - Determination of shear behaviour of structural bonds - Part 2: Thick adherends shear test.
[32] DNV-GL-ST-C502: Offshore concrete structures, Norway, 2018.
[33] DIN EN 196–1:2016–11, Prüfverfahren für Zement_- Teil_1: Bestimmung der Festigkeit; Deutsche Fassung EN_196–1:2016. Berlin: Beuth Verlag GmbH. 〈https://doi.org/10.31030/2482416〉.
[34] DIN EN 10025–1:2005–02, Warmgewalzte Erzeugnisse aus Baustählen_- Teil_1: Allgemeine technische Lieferbedingungen; Deutsche Fassung EN_10025–1:2004. Berlin: Beuth Verlag GmbH. 〈https://doi.org/10.31030/9429825〉.
[35] DIN EN ISO 15711:2005–03, Beschichtungsstoffe_- Bestimmung des Widerstandes gegen kathodische Enthaftung von Beschichtungen in Meerwasser (ISO_15711: 2003); Deutsche Fassung EN_ISO_15711:2004. Berlin: Beuth Verlag GmbH. 〈https://doi.org/10.31030/9608654〉.
[36] M.K. Budzik, M. Wolfahrt, P. Reis, M. Kozłowski, J. Sena-Cruz, L. Papadakis, et al., Testing mechanical performance of adhesively bonded composite joints in engineering applications: an overview, J. Adhes. 98 (14) (2022) 2133–2209, https://doi.org/10.1080/00218464.2021.1953479.